AGU PUBLICATIONS

Geophysical Research Letters

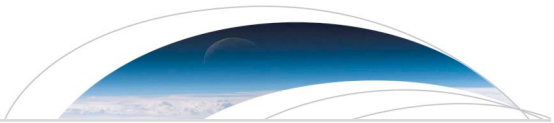

RESEARCH LETTER

10.1002/2015GL067254

Key Points:

- The North Atlantic deep ocean heat content significantly increased without atmospheric heat uptake
- Forty percent of such increase below 300 m occurred quickly in the mid-2000s at ENA modal waters formation area
- ENA modal waters transformation also aided a circulation shift with far reaching consequences

Supporting Information:

- Supporting Information S1

Correspondence to:
R. Somavilla,
raquel.somavilla@gi.ieo.es

Citation:
Somavilla, R., C. González-Pola, U. Schauer, and G. Budéus (2016), Mid-2000s North Atlantic shift: Heat budget and circulation changes, *Geophys. Res. Lett.*, *43*, 2059–2068, doi:10.1002/2015GL067254.

Received 1 DEC 2015
Accepted 8 FEB 2016
Accepted article online 10 FEB 2016
Published online 2 MAR 2016

Mid-2000s North Atlantic shift: Heat budget and circulation changes

R. Somavilla[1], C. González-Pola[1], U. Schauer[2], and G. Budéus[2]

[1] Instituto Español de Oceanografía, C.O. de Gijón, [2] Alfred Wegener Institute, Helmholtz Centre for Polar and Marine Research, Bremerhaven, Germany

Abstract Prior to the 2000s, the North Atlantic was the basin showing the greatest warming. However, since the mid-2000s during the so-called global warming hiatus, large amounts of heat were transferred in this basin from upper to deeper levels while the dominance in terms of atmospheric heat capture moved into the Indo-Pacific. Here we show that a large transformation of modal waters in the eastern North Atlantic (ENA) played a crucial role in such contrasting behavior. First, strong winter mixing in 2005 transformed ENA modal waters into a much saltier, warmer, and denser variety, transferring upper ocean heat and salt gained slowly over time to deeper layers. The new denser waters also altered the zonal dynamic height gradient reversing the southward regional flow and enhancing the access of saltier southern waters to higher latitudes. Then, the excess salinity in northern regions favored additional heat injection through deep convection events in later years.

1. Introduction

More than 90% of the increasing radiative forcing imbalance is reflected as global ocean warming [*Alexander et al.*, 2013]. In the view of that, the deceleration of the upper ocean heat storage since the mid-2000s [*Levitus et al.*, 2009; *Balmaseda et al.*, 2013; *Cheng and Zhu*, 2015] has instigated an active search for the "missing heat" in the deep ocean [*Meehl et al.*, 2011; *Trenberth and Fasullo*, 2010; *Katsman and van Oldenborgh*, 2011; *Balmaseda et al.*, 2013; *Kosaka and Xie*, 2013]. The enhanced downward heat transfer necessary for this vertical heat redistribution has been proposed to be related to the hiatus in global warming, although the hiatus started earlier and lasted for the 15 years period 1998–2013 [*Trenberth et al.*, 2014; *Trenberth*, 2015; *Karl et al.*, 2015]. Two natural mechanisms have been proposed to explain the deceleration of the rise in global mean surface temperature and the efficient transfer of heat to the deep ocean: (I) the intensification of zonal winds causing La Niña-like conditions in the tropical Pacific [*Meehl et al.*, 2011; *Trenberth and Fasullo*, 2010; *Katsman and van Oldenborgh*, 2011; *Balmaseda et al.*, 2013; *Kosaka and Xie*, 2013] and (II) decadal variations in the strength of deep convection and currents in the North Atlantic [*Meehl et al.*, 2011; *Katsman and van Oldenborgh*, 2011; *Chen and Tung*, 2014; *Drijfhout et al.*, 2014]. Regarding the first mechanism, modeling simulations show that La Niña surface cooling in the eastern and central tropical Pacific can decrease the rate of increase in atmospheric temperature (although the similarity of observed and simulated deceleration is still debated [*Trenberth*, 2015; *Karl et al.*, 2015]) and induce an anomalous heat flux into the ocean [*Kosaka and Xie*, 2013; *England et al.*, 2014; *Balmaseda et al.*, 2013]. Associated to this anomalous heat flux into the ocean, subsurface heat uptake in the western tropical Pacific and Indian Oceans occurs [*Goddard*, 2014; *England et al.*, 2014; *Meehl et al.*, 2013; *Lee et al.*, 2015] mostly above 300 m (see Figure S1 in the supporting information) [*Chen and Tung*, 2014, Figures 1 and 3; *Nieves et al.*, 2015], thus not largely involving transfer of heat into the deep ocean.

Regarding the second mechanism, vertical heat inventories of the North Atlantic show notable heat transfer from the upper (0–300 m) to intermediate (300–700 m) and deep (>700 m) layers since the mid-2000s (see Figure S1 and corresponding comments) [*Alexander et al.*, 2013, Figure 3.1; *Chen and Tung*, 2014, Figure 6; *Williams et al.*, 2014, Figure 1c]. Such recent downward heat transfer follows decades of sustained surface warming and increasing ocean heat content in the basin [*Drijfhout et al.*, 2014; *Häkkinen et al.*, 2015; *Williams et al.*, 2014; *Durack et al.*, 2014]. However, concomitant with the downward heat export after the mid-2000s, the increase in ocean heat content in the upper 2000 m of the North Atlantic paused [*Chen and Tung*, 2014, Figures 1 and 3; *Häkkinen et al.*, 2015, Figure 1], making the bulk rate of change of

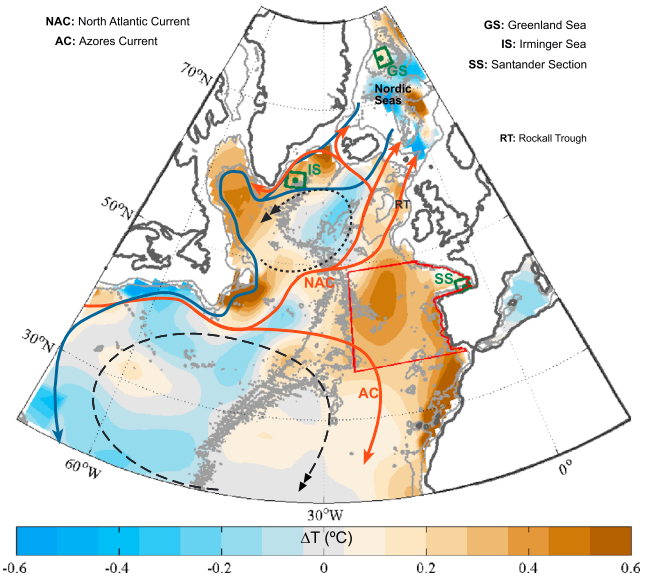

Figure 1. Warming pattern in the North Atlantic at middepth. Temperature differences (ΔT in color, °C) in the 300–700 m layer between the 2007–2012 and the 1997–2002 periods (i.e., average values are estimated for each time range). Figure 1 is the zoom into the North Atlantic in Figure S1 Ocean Reanalysis System 4 (ORAS4) (d) (see Figure S1 procedure description for details). Brown colors indicate warming. Arrows represent (in red) warm and salty upper water currents, (in dark blue) cold and fresh deep water currents, (in black, dotted) the subpolar gyre, and (in black, dashed) the subtropical gyre. Deep convection sites in the Irminger and Greenland Seas as well as the position of the Santander standard section in the Bay of Biscay are marked by green squares. Midlatitudes in the Eastern North Atlantic (ml-ENA), considered as the oceanic area including the mode water formation area of the Eastern North Atlantic Central Water (ENACW) and the oceanic waters of the Bay of Biscay and surrounding the Iberian Peninsula to North Africa as in *Somavilla et al.* [2009] is bounded by a red box.

ocean heat content per unit area in the basin almost zero. Bulk rates of change in ocean heat content per unit area are considered an estimation of the ocean heat uptake (Q, W m^{-2}) at ocean basin scales [e.g., *Mauritzen et al.*, 2012; *Guemas et al.*, 2013; *Chen and Tung*, 2014]. Changes in ocean circulation can generate ocean heat content anomalies of opposite signs between different ocean layers and regions (e.g., subtropical versus subpolar gyre), but the anomalies compensate when integrated at ocean basin scales and decadal timescales [*Lozier et al.*, 2008; *Mauritzen et al.*, 2012]. Therefore, one can conclude that the heat redistribution in the North Atlantic since the mid-2000s as a whole has apparently occurred without extra heat uptake from the atmosphere. Overall, during the past decade, different basins have played contrasting roles on the Earth's atmosphere-ocean heat budget distribution. In particular, the North Atlantic would not have contributed notably as in previous decades to atmospheric heat uptake, in contrast to that observed in the tropical Pacific and Southern Oceans [*Roemmich et al.*, 2015], but to the quick transfer of heat accumulated during the previous decades in the upper layers to the deep ocean. What are the causes for this shift?

Deep convection in the subpolar North Atlantic under high-salinity conditions might account for the quick transfer of heat to the deep ocean [*Chen and Tung*, 2014]. According to these authors, recent high-salinity conditions may be caused by a strengthening of the Atlantic Meridional Overturning Circulation (AMOC). Agreeing that high salinity in deep convection regions favors heat transfer to the deep ocean [*Mauritzen et al.*, 2012], two objections can be drawn from this overall view. First, available observational records do not show a strengthening of the AMOC [*Kanzow et al.*, 2010; *Smeed et al.*, 2014; *Drijfhout et al.*, 2014] but suggests a sustained weakening [*Srokosz and Bryden*, 2015]. Second, deep convection in the subpolar North Atlantic is restricted to the Labrador and Irminger Seas (see Figure 1), but far from these prominent deep ocean ventilation sites, ocean observations seem to show the largest deep ocean heat uptake at midlatitudes in the Eastern North Atlantic (Figure 1) [*Desbruyères et al.*, 2014].

Here we reexamine the mechanism responsible for the quick transfer of ocean heat from upper to deeper layers in the North Atlantic focusing on the role of ENA modal waters.

2. Data Sets

High-quality hydrographic data with global coverage are required for providing observational evidence to the mid-2000s shift in the North Atlantic. These data are obtained from regularly observed hydrographic sections, which are affected by gaps in coverage both in time and space. To overcome this issue, we combined standard hydrographic observations (salinity and temperature profiles) at oceanographic sections regularly maintained in the Bay of Biscay and the Greenland Sea (see Figure 1) with other data sets that offer more global coverage such as Argo floats, global-gridded ocean reanalysis (European Centre for Medium-Range Weather Forecasts Ocean Reanalysis System 4, ORAS4) and objective analysis (Met Office Hadley Centre monthly objective analysis, EN4, and World Ocean Database 2001, WOA01).

Along the work, temperature and salinity time series from oceanographic sections are systematically presented together with those constructed from Argo floats and reanalysis data. In this manner, we prove that the changes detected at oceanographic sections are representative of larger oceanic areas (e.g., Figures 2 and 5), and it serves as an important validation for both Argo floats and gridded data sets affected by factors such as changes in observation coverage around 2005 [*Roemmich et al.*, 2015], contamination from model errors in ocean reanalysis data [*Balmaseda et al.*, 2013], or the gap-filling strategy in climatological data [*Cheng and Zhu*, 2015]. With a similar purpose of increasing the reliability of individual data sets, warming/cooling and saltening/freshening maps obtained from different gridded data are compared (Figures S1 and S2). Thus, we increase the confidence of the enhanced warming at midlatitudes in the Eastern North Atlantic as shown in Figure 1, since similar warming distributions showing enhanced heat uptake at midlatitudes in the ENA and surrounding the subpolar North Atlantic margins are observed in other gridded products (Figure S1 based on EN4; Figure 3c in *Chen and Tung* [2014] based on Ishii data; Figure 4 to 6 in *Häkkinen et al.* [2013] based on NOAA/National Oceanographic Data Center database; Figure 3.1 on the Intergovernmental Panel on Climate Change report [*Alexander et al.*, 2013] constructed from an update of the annual analysis of *Levitus et al.* [2009]). A complete description of the data sets, methods, and further details are included in the supporting information.

3. Transformation of North-East Atlantic Modal Waters in 2005 and Implications for Basin-Scale Circulation

The winter of 2005 was exceptionally cold and dry in southwestern Europe [*Shein*, 2006; *Somavilla et al.*, 2009]. That year, the ocean surface at midlatitudes in the Eastern North Atlantic (ml-ENA, see Figure 1 for geographical reference) experienced the highest densification (buoyancy loss) since the 1960s, causing the winter mixed layer to reach very deep levels likely unprecedented for decades [*Somavilla et al.*, 2009, 2011]. The induced deep convective mixing resulted in homogeneization of properties of the water column from the surface to density levels of $\sigma_\theta = 27.2–27.3$ kg m^{-3}, at depth ranges of 350–500 m, well beyond the normal air-sea interaction extent at the core of ENACW ($\sigma_\theta = 27.1–27.2$ kg m^{-3}). This mixing of (warmer and saltier) upper water and (colder and fresher) modal waters made the upper waters colder (−0.4°C), creating a denser (+0.1 kg m^{-3}), warmer (+0.23°C), and more saline (+0.015) type of ENACW (Figures 2 and S1) [*Somavilla et al.*, 2009].

Such temperature increase at the ENACW core (+0.23°C) resulted in a sudden heat content increase of $2.4 \cdot 10^8$ J m^{-2} for the 350–500 m layer ($3.9 \pm 0.6 \cdot 10^8$ J m^{-2} for the 300–700 m layer, Table S1). This suggests that 70% of the estimated $5.8 \cdot 10^8$ J m^{-2} of heat gained slowly but persistently between 1994 and 2005 in the shallower levels (0.7°C in the 100–300 m layer, Table S1 and Figure 2a) was transferred into a denser variety of mode waters through the extreme winter mixing. In addition, considering that such heat injection took place during winter 2005, the heat uptake (Q) at intermediate depths would be 30 W m^{-2} (5 W m^{-2} for the 300–700 m layer), between 65 and 100 times faster than the average ocean heat uptake at such intermediate depths (300–700 m) between 2000 and 2010 (see Table S1). Note that the heat uptake at intermediate depths originates from the heat transfer from the upper layers and not from the atmosphere. Forced by atmospheric cooling, the convective mixing would have released heat to the atmosphere (see comments in Table S1 for additional information).

Most of the enhanced warming observed at intermediate depths at ml-ENA shown in Figure 1 (+0.33°C gained between 1997 and 2012) is explained by the increase in the modal waters during the winter of 2005 (+0.23°C). The estimated overall heat content increase in the region is 1.2×10^{21} J and accounts for 44% of the total heat content increase at intermediate depths in the North Atlantic from 36° to 65°N from 1997 to 2012 (Table S2).

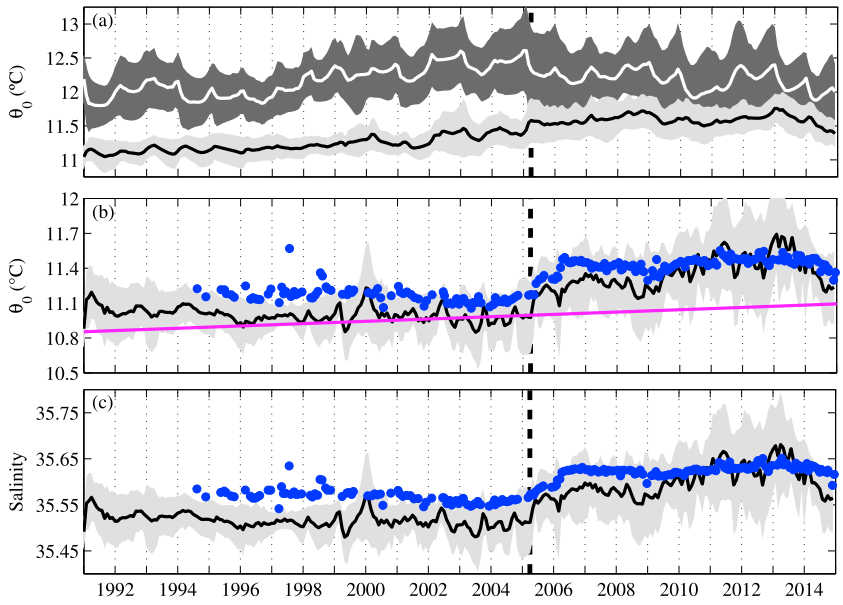

Figure 2. Strong mixing-induced deep ocean heat injection at ml-ENA. (a) Mean temperature (white line) between the shallower winter mixed layer depth achieved in warm winters and the ENACW upper bound (100–300 m) and (black line) in the depth range of the ENACW core (300–550 m) in the ENACW formation area (43°–48°N, 10°–20°W) obtained from ORAS4 Reanalysis data set. Gray shaded regions represent ± 2 standard deviation from the spatial average. (b and c) Same as Figure 2a but for temperature and salinity at σ_θ = 27.2–27.3 kg m^{-3} (corresponding to the +0.1 kg m^{-3} 2005 denser ENACW core). The blue circles indicate temperature and salinity at σ_θ = 27.2–27.3 kg m^{-3} as recorded at station 7 of the Santander standard section (Figure 1). The magenta line in Figure 2b shows the background average warming trend (+0.1°C decade^{-1}) at the intermediate depth (300–700 m) for the global ocean (Table S1).

Evidence suggests that this extreme winter mixing episode may have contributed to the deep ocean heat injection at higher latitudes by inducing ocean circulation changes that enabled northward propagation of the relatively salty ENACW. ml-ENA climatological circulation charts and specific studies indicate slow southward flow west of the Bay of Biscay and Iberia [*Pollard et al.*, 1996; *Pingree*, 1993; *Reid*, 1994] (Figure 3a). Enhanced mixing in 2005 altered the regional climatological density structure. In the climatology, the 27.15 isopycnal became shallower from the mid-Atlantic eastward and peaked at about 18°W, beyond which it deepened slowly. After winter 2005, the isopycnals became shallower all the way against the European margin (Figures 3b–3d). The associated zonal dynamic height sections were thus altered, and the zonal dynamic height slope eastward of 22°W changed from almost flat or negative to positive (Figures 3e–3g). Hence, the associated meridional flow shifts from southward to northward. Estimated as the geostrophic meridional current between 22° and 12°W ($v_g = \Delta\Phi/fL$, where $\Delta\Phi$ is the difference between the dynamic height at 12°W and 22°W, f the Coriolis parameter, and L the distance between the two longitudes), the meridional current after 2005 estimated from the mean filtered dynamic height from Argo floats is +0.7 cm s^{-1} (northward) with respect to −0.4 cm s^{-1} (southward) estimated from WOA01 climatological dynamic height (with reference level at 1500 m both for Argo floats and WOA01 data). ORAS4 meridional current data show a comparable northward reversal of the flow centered at 18°W from 2005 to 2010 (mean value = +1 cm s^{-1}, maximum value = +3 cm s^{-1}) with respect to its southward direction (mean value = −0.5 cm s^{-1}, maximum value = −3 cm s^{-1}) from 1990 to 2005 (see Figure S3). The inversion of the zonal dynamic height slope is a robust feature (e.g., with reference level at 1000 m, the meridional current after 2005 estimated from Argo floats is +0.6 cm s^{-1} (northward) with respect to −0.35 cm s^{-1} (southward) estimated from WOA01 climatological dynamic height) as also observed in ORAS4 meridional current (Figure S3). A similar flow reversal was predicted by a sensitivity experiment in a global ocean circulation model, and anomalous northward advection of salt was obtained as a result of surface cooling at 45°N in the ENA [*Sévellec et al.*, 2008].

It is worth noting that the maximum water exchange between the subtropical and the subpolar gyres occurs at a density level of σ_θ = 27.2–27.4 kg m^{-3} [*Brambilla and Talley*, 2006]. Thus, the +0.1 kg m^{-3} denser core of ENACW (σ_θ = 27.2–27.3 kg m^{-3} after 2005) might easily get incorporated to the major branch of the North

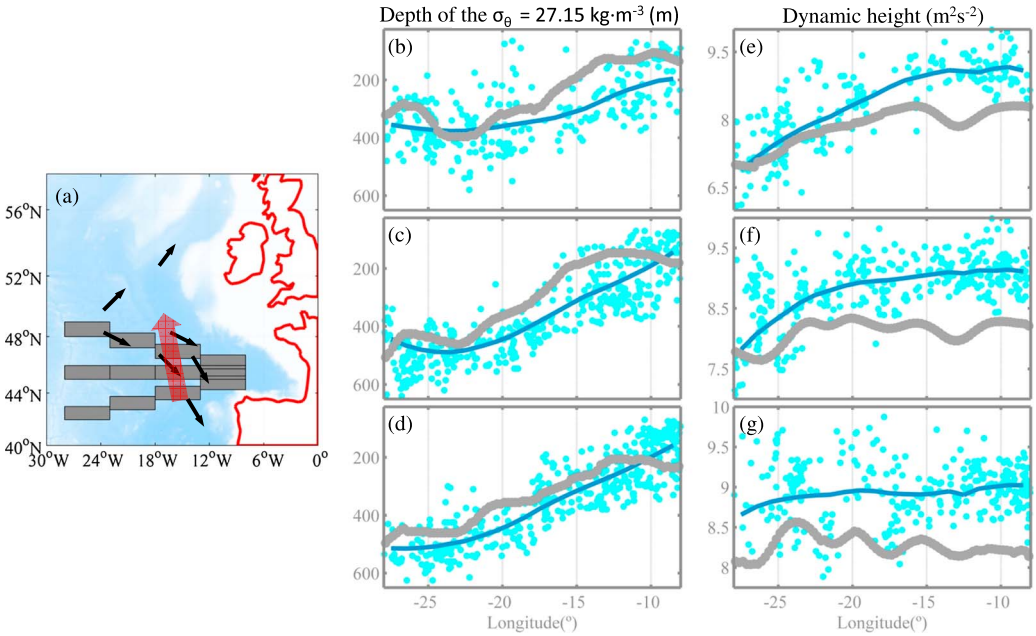

Figure 3. Flow reversal in ENACW. (a) Map of the Northeast Atlantic showing the location of the NW-SE, W-E, and SW-NE sections across the ENACW formation area for which the data are shown in Figures 3b–3g. (b–d) Location of the σ_θ = 27.15 at the NW-SE, E-W, and SW-NE sections marked in Figure 3a based on WOA01 climatological data (grey) and available Argo floats in the corresponding section between 2005 and 2010 (cyan). The blue line indicates the mean filtered value of all the Argo floats each 2° of longitude. (e–g) Idem for the dynamic height between 300 and 1500 m (see section 2.3 in the supporting information for details). Black arrows in Figure 3a indicate the southward flow west of the Bay of Biscay based on *Pollard et al.* [1996], inferred in Figures 3e–3g from the climatological data (grey dots); and the red arrow indicates the reversed flow after 2005, shown in Figures 3e–3g by Argo floats (blue line).

Atlantic current flowing northward. The anomalous northward flow of salty ENACW is also inferred directly from large-scale hydrography (see Figure 4b) as will be described in detail in the next section.

Due to the weak circulation and dominance of mesoscale activity in the ml-ENA region, finding direct evidence of a flow reversal as the one inferred from dynamic height and reanalysis current data is difficult. Argo-based deep displacements [*Ollitrault and Rannou*, 2013] are an available source, and luckily, a number of floats drifting at ENACW levels were active in the region (see Figure S4). The outcome from the analysis of their Lagrangian displacements is not inconsistent with the flow reversal but cannot be considered conclusive.

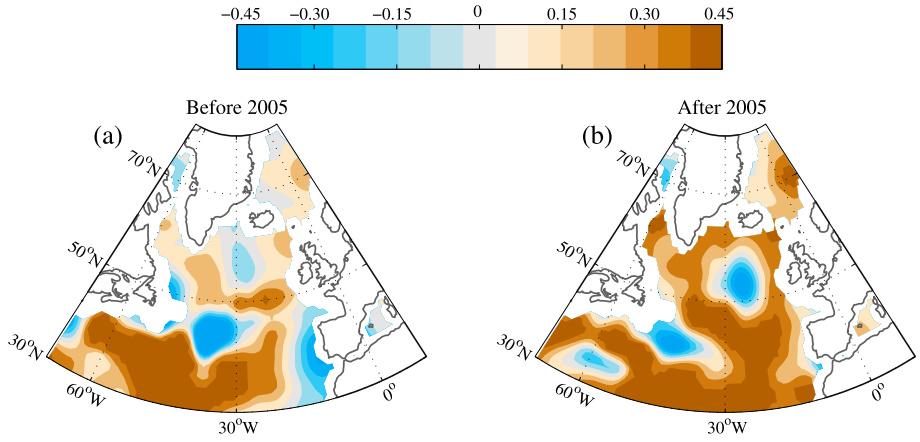

Figure 4. Increasing salinities at middepths after 2005. Salinity difference (ΔS in color) in the 300–700 m layer between (a) the 2002–2005 and the 1997–2002 periods and (b) the 2007–2012 and the 1997–2002 periods based on EN4 data set (i.e., average values are estimated for each time range). Figure 4 is the zoom into the North Atlantic in Figure S2 EN4 (c and d) (see Figure S2 procedure description for details). Brown colors indicate increasing salinities.

4. Increasing Salinities and Deep Ocean Heat Injection at Higher Latitudes

Upper water temperature and salinity in the subpolar gyre and the Nordic Seas increased since early the 2000s; this tendency is attributed to the arrival of warmer and saltier western subtropical waters caused by the contraction of the subpolar gyre [*Hátún et al.*, 2005; *Woollings*, 2011]. Though the higher salinities peaking between 2007 and 2010 in these areas (see Figure 4b) [*Holliday et al.*, 2008; *Beszczynska-Möller and Dye*, 2013; http://ocean.ices.dk/iroc/] would be consistent with a higher transport of western subtropical waters, that higher transport does not account for the drop in nutrient concentration in the eastern subpolar North Atlantic (Rockall Trough, Figure 1) observed from 2007 onward [*Johnson et al.*, 2013]. This drop in nutrient concentration is explained by a higher contribution of ENACW in the area [*Johnson et al.*, 2013], thus adding further evidence in support of the circulation reversal previously described. The enhanced northward flow in the ENA would have reinforced the northwestward retreat of the subpolar front [*Häkkinen et al.*, 2013], broadening the passage for both ENACW and western subtropical waters toward the north (see Figure 4b). Both the eastern and western North Atlantic Central Water types have the potential to increase temperature and salinity at higher latitudes. However, ENACW are saltier than western waters arriving at the eastern subpolar North Atlantic [*Johnson et al.*, 2013; *Häkkinen et al.*, 2013], providing an alternative explanation for the highest-salinity anomalies observed between 2007 and 2010 in the subpolar North Atlantic and Nordic Seas.

Assuming mean anomaly propagation speeds of 2 to 3 cm s^{-1} [*Larsen et al.*, 2012; *Holliday et al.*, 2008], a lag of 2 to 5 years is expected for the salinity anomaly (from the ml-ENA) to reach first the eastern subpolar North Atlantic and then the western subpolar gyre and northern Nordic Seas. In these areas, the arrival of salty southern waters due to the circulation shift in the ml-ENA would have contributed to the high-salinity conditions required for deep ocean heat uptake through density compensated anomalies [*Mauritzen et al.*, 2012; *Chen and Tung*, 2014] without requiring an increase of the AMOC as suggested by *Chen and Tung* [2014]. Such circulation shift and enhanced northward flow in the ml-ENA do not seem to contradict the observed weakening of AMOC [*Srokosz and Bryden*, 2015]. Indeed, a strong northward flow east of 22°W and south of 48°N in the a priori recirculation area at the 'OVIDE' section crossing the North Atlantic from Portugal to Greenland was observed in 2006, coincident with the lowest AMOC measured through the section between 1997 and 2010 [*Mercier et al.*, 2013]. Consistent with the aforementioned spreading timescale and presence of the saltiest upper waters after 2007 in these areas, the heat and salt uptake below 700 m in the subpolar gyre and the Nordic Seas increased after 2007 (Figures S1 and S2), coinciding with more intensive deep convection activity in both the subpolar gyre (Irminger and Labrador seas, [*Yashayaev and Loder*, 2009; *Kieke and Yashayaev*, 2015; *de Jong et al.*, 2012; *Piron et al.*, 2015]) and Nordic Seas (Greenland Sea, [*Beszczynska-Möller and Dye*, 2013]). After years of sustained warming and increasing salinity in the upper layers, the first deep convection events at each of these sites resemble the ENACW transformation in 2005. In the deep water formation region of the Greenland Sea, a strong mixing-induced deep ocean heat injection event occurred through density compensated anomalies in 2008 (Figure 5). Upper ocean salinity in this region had been increasing since the mid-1990s, and the 2008 winter cooling made the surface waters dense enough to trigger deep convection with temperature and salinity higher than typical values (Figure S5). As a consequence of the overturning, the heat and salt gained slowly over time by the upper layers were directly injected to great depths, with a resulting sudden temperature and salinity increase of 0.16°C and 0.01, respectively (Figures 5c and 5d). With a less stratified water column, convection occurred at greater depths in the subsequent years as compared to previous decades in the Greenland Sea [*Beszczynska-Möller and Dye*, 2013]. Coincident with the arrival of highly saline waters in the upper layers of the subpolar gyre, a strong winter mixing occurred in the Irminger Sea in 2007 [*Piron et al.*, 2015] and induced deep ocean heat uptake. Figures 5a and 5b show sudden increases in temperature (0.15°C) and salinity (0.01) at depth, related to this event. As in the Greenland Sea, subsequent deep convection events followed in later years (2008, 2009, and 2012) [*de Jong et al.*, 2012; *Piron et al.*, 2015]. Finally, coinciding with the arrival of highly saline waters in the upper levels, deep convection has reached levels deeper than 1700 m in the Labrador Sea in 2008 after more than a decade of weak convection, being repeated in 2012 and 2014 [*Kieke and Yashayaev*, 2015]. As in the Greenland and Irminger Seas, the first deep convection events appear to be associated with downward transfer of heat and salt [see *Yashayaev and Loder*, 2009, Figure 2a; *Kieke and Yashayaev*, 2015, Figure 4b]. In general, the step-like temperature increases at depth at deep convection sites caused by the strong mixing-induced heat injection events are equivalent to heat uptake pulses between 16 and 25 W m^{-2}, which is between 50 and 100 times faster than the average heat uptake below 700 m in the global ocean (see Table S1). As in the ml-ENA, concurrent with the deep ocean heat injection, the deep convective mixing events would have released heat to the atmosphere,

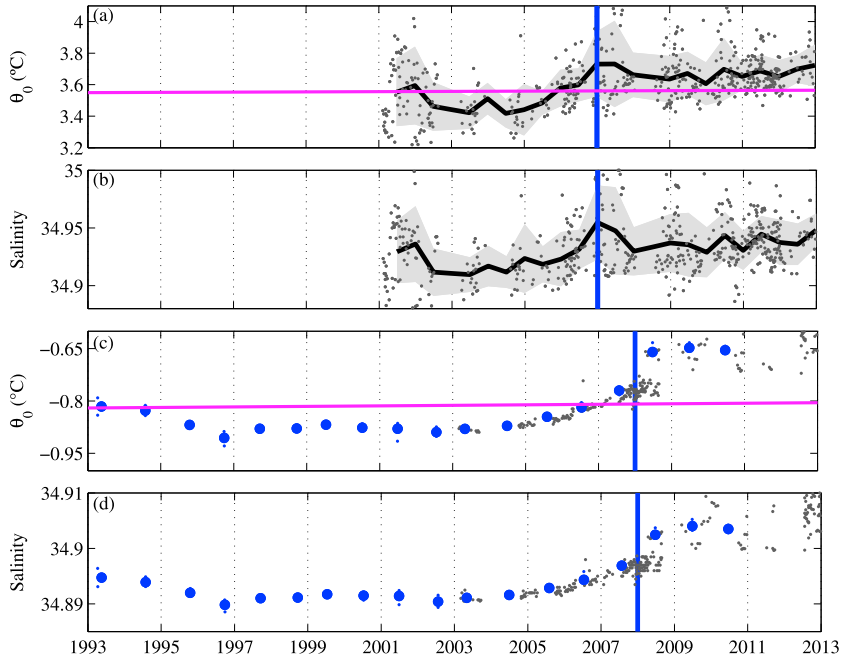

Figure 5. Strong mixing-induced deep ocean heat injection events at deep convection sites. Deep (a) temperature and (b) salinity (1400–1600 dbar, σ_θ = 27.78–27.8 kg m^{-3}) in the Irminger Sea (60°–62°N; 35°–40°W, green square in Figure 1) based on Argo data. Grey dots indicate vertically averaged Argo temperature and salinity values in the pressure range of interest from individual profiles. Gray shaded regions represents ±2 standard deviation from the spatial average (black). Deep (c) temperature and (d) salinity (1500–1800 dbar, σ_θ = 28.058–28.062 kg m^{-3}) in the Greenland Sea (74°–76°N; 0°–6°W, see Figure 1). Blue circles indicate vertically and spatially averaged conductivity-temperature-depth (CTD) casts in the area and pressure range of interest and grey dots vertically averaged temperature and salinity of individual Argo floats. The magenta line in Figures 5a and 5c shows the background global ocean average warming trend below 700 m (+0.015°C decade^{-1}) (Table S1). Blue lines highlight the years 2007 (in Figures 5a and 5b) and 2008 (in Figures 5c and 5d).

favoring deceleration of the North Atlantic heat uptake from the atmosphere, as apparently observed since the mid-2000s [*Chen and Tung*, 2014; *Häkkinen et al.*, 2015] (see section 1 for details).

5. Further Remarks

The primary cause of the extremely cold winter in 2005 in the ml-ENA was the occurrence of atmospheric blocking anomalies in the ENA. In addition to its effects on ocean circulation described in section 2 (i.e., regional enhanced mixing altering the large-scale density structure), blocking anomalies in the ENA generate a dipole of temperature anomalies between Europe (cold) and Greenland (warm) associated with a strong northward meridional atmospheric flow [*Barriopedro et al.*, 2008] with a potential to reinforce large-scale ocean circulation changes. Blocking anomalies over the ENA occurred previously in the late 1950s and 1960s and extreme winter mixing events (similar to that in 2005) were observed in the area [*Somavilla et al.*, 2009, 2011; *Häkkinen et al.*, 2011]. Under these conditions, enhanced northward flow of ENACW may have occurred and contributed (along with western subtropical waters) to the intrusion of warmer and saltier waters into the eastern subpolar North Atlantic and Nordic Seas during the 1960s [*Holliday et al.*, 2008]. A contraction of the subpolar gyre [*Hátún et al.*, 2005], as well as enhanced heat uptake by the subpolar gyre through density-compensated temperature anomalies [*Mauritzen et al.*, 2012; *Chen and Tung*, 2014; *Häkkinen et al.*, 2013; *Williams et al.*, 2014] are documented for that period. The heat uptake in the 1960s had smaller amplitude compared to the 2005 event, and this may be related to the sustained warming trend in the global upper ocean in the few decades prior to 2005.

The ultimate driver for the occurrence of blocking anomalies at midlatitudes is under debate [*Kintisch*, 2014]. Both warmer Arctic and tropical Pacific have been associated with a wavier jet stream responsible for an increase in blocking events in the North Atlantic and higher frequency of extreme weather events in general [*Francis and Vavrus*, 2012; *Trenberth et al.*, 2014]. The blocking pattern developed in winter 2005 in the

ENA region is not inconsistent with natural climate variability [*Barnes et al.*, 2014; *Barriopedro et al.*, 2008]. However, overall global warming is expected to affect the development of such atmospheric features [*Alexander et al.*, 2013] as well as the subsequent ocean response. Estimating the global significance of ocean heat transfer from upper to deeper levels by the mechanism described here requires a better model representation of the frequency and duration of wintertime blocking events, which have been underestimated in most global climate models thus far [*Hov et al.*, 2013].

6. Conclusions

Since the mid-2000s, in contrast to the enhanced ocean heat uptake observed in other ocean basins, the North Atlantic deep ocean heat content has significantly increased without apparently intervening ocean heat uptake from the atmosphere. About 40% of the increase in deep ocean heat content increase below 300 m is centered at midlatitudes in the Eastern North Atlantic and occurred relatively quickly around the mid-2000s far from prominent deep ocean ventilation sites. We suggest that a sequence of connected strong mixing-induced heat injection events originating from this region triggered large transfer of heat from upper to deeper ocean layers, implying a deceleration or halt of the North Atlantic heat uptake from the atmosphere. A large transformation of modal water masses in the Eastern North Atlantic in the winter of 2005 played a major role in the observed quick transfer of heat from upper to deep ocean layers but also aided a reverse of the southward circulation of saltier waters from the eastern side of the temperate Atlantic with far reaching consequences; the northward flow of saltier waters into the subpolar North Atlantic and Nordic Seas favored additional heat injection through deep convection events in later years. Thus, we agree that existing high-salinity conditions in the late 2000s in areas of deep convection have aided heat transfer to the deep ocean, but the suggestion that an increase of the AMOC is behind such salinity increase is not supported by observations. A greater influence of the saltier ENACW and broadened passage for both ENACW and western subtropical waters toward the north appears to be a more plausible explanation. Anomalous atmospheric patterns such as the one behind this shift are not unique to the last decade, although they may have been exacerbated under global warming.

Acknowledgments
The authors wish to thank two anonymous reviewers for valuable and helpful comments on the manuscript. Hydrographic measurements (salinity, temperature, and pressure from CTD data) from the Santander section used in this study are available on request at http://indamar.ieo.es and those from the Greenland Sea are freely available from the Pangaea database (www.pangaea.de). R. Somavilla is supported by a Marie Curie Clarín Cofund grant (AC B-1431). Support for this study was provided by the Principado de Asturias (GRUPIN14-144: GIDEP: Grupo de Investigacion de Dinamica del Ecosistema Planctonico).

References

Alexander, L. V., et al. (2013), Working group I contribution to the IPCC Fifth Assessment Report Climate Change 2013: The Physical Science Basis. [Available at www.ipcc.ch/report/ar5/wg1/.]

Balmaseda, M. A., K. E. Trenberth, and E. Kalén (2013), Distinctive climate signals in reanalysis of global ocean heat content, *Geophys. Res. Lett.*, *40*, 1754–1759, doi:10.1002/grl.50382.

Barnes, E. A., E. Dunn Sigouin, G. Masato, and T. Woollings (2014), Exploring recent trends in Northern Hemisphere blocking, *Geophys. Res. Lett.*, *41*, 638–644, doi:10.1002/2013GL058745.

Barriopedro, D., R. García-Herrera, and R. Huth (2008), Solar modulation of Northern Hemisphere winter blocking, *J. Geophy. Res.*, *113*, D14118, doi:10.1029/2008JD009789.

Beszczynska-Möller, A., and S. R. Dye (2013), ICES report on ocean climate 2012, *ICES Coop. Res. Rep. 321*, Int. Counc. for the Explor. of the Sea, Copenhagen.

Brambilla, E., and L. D. Talley (2006), Surface drifter exchange between the North Atlantic subtropical and subpolar gyres, *J. Geophys. Res.*, *111*, C07026, doi:10.1029/2005JC003146.

Chen, X., and K. K. Tung (2014), Varying planetary heat sink led to global-warming slowdown and acceleration, *Science*, *345*(6199), 897–903, doi:10.1126/science.1254937.

Cheng, L., and J. Zhu (2015), Influences of the choice of climatology on ocean heat content estimation, *J. Atmos. Oceanic Technol.*, *32*, 388–394, doi:10.1175/JTECH-D-14-00169.1.

de Jong, M. F., H. M. van Aken, K. Våge, and R. S. Pickart (2012), Convective mixing in the central Irminger Sea: 2002–2010, *Deep Sea Res., Part I*, *63*, 36–51, doi:10.1016/j.dsr.2012.01.003.

Desbruyères, D., E. McDonagh, B. King, F. Garry, A. Blaker, B. Moat, and H. Mercier (2014), Full-depth temperature trends in the Northeastern Atlantic through the early 21st century, *Geophys. Res. Lett.*, *41*, 7971–7979, doi:10.1002/2014GL061844.

Drijfhout, S. S., A. T. Blaker, S. A. Josey, A. J. G. Nurser, B. Sinha, and M. A. Balmaseda (2014), Surface warming hiatus caused by increased heat uptake across multiple ocean basins, *Geophys. Res. Lett.*, *41*, 7868–7874, doi:10.1002/2014GL061456.

Durack, P. J., P. J. Gleckler, F. W. Landerer, and K. E. Taylor (2014), Quantifying underestimates of long-term upper ocean warming, *Nat. Clim. Change*, *4*(11), 999–1005, doi:10.1038/nclimate2389.

England, M. H., S. McGregor, P. Spence, G. A. Meehl, A. Timmermann, W. Cai, A. S. Gupta, M. J. McPhaden, A. Purich, and A. Santoso (2014), Recent intensification of wind-driven circulation in the Pacific and the ongoing warming hiatus, *Nat. Clim. Change*, *4*, 222–227, doi:10.1038/nclimate2106.

Francis, J. A., and S. J. Vavrus (2012), Evidence linking Arctic amplification to extreme weather in mid-latitudes, *Geophys. Res. Lett.*, *39*, L06801, doi:10.1029/2012GL051000.

Goddard, L. (2014), Heat hide and seek, *Nat. Clim. Change*, *4*(3), 158–161, doi:10.1038/nclimate2155.

Guemas, V., F. J. Doblas-Reyes, I. Andreu-Burillo, and M. Asif (2013), Retrospective prediction of the global warming slowdown in the past decade, *Nat. Clim. Change*, *3*, 649–653, doi:10.1038/nclimate1863.

Hátún, H., A. B. Sandø, H. Drange, B. Hansen, and H. Valdimarsson (2005), Influence of the Atlantic subpolar gyre on the thermohaline circulation, *Science*, *309*(5742), 1841–1844, doi:10.1126/science.1114777.

Häkkinen, S., P. B. Rhines, and D. L. Worthen (2011), Atmospheric blocking and Atlantic multidecadal ocean variability, *Science*, *334*(6056), 655–659, doi:10.1126/science.1205683.

Häkkinen, S., P. B. Rhines, and D. L. Worthen (2013), Northern North Atlantic sea surface height and ocean heat content variability, *J. Geophys. Res. Oceans*, *118*, 3670–3678, doi:10.1002/jgrc.20268.

Häkkinen, S., P. B. Rhines, and D. L. Worthen (2015), Heat content variability in the North Atlantic Ocean in ocean reanalyses, *Geophys. Res. Lett.*, *42*, 2901–2909, doi:10.1002/2015GL063299.

Holliday, P. N., et al. (2008), Reversal of the 1960s to 1990s freshening trend in the northeast North Atlantic and Nordic Seas, *Geophys. Res. Lett.*, *35*, L03614, doi:10.1029/2007GL032675.

Hov, Ø., et al. (2013), *Extreme Weather Events in Europe: Preparing for Climate Change Adaptation*, Norwegian Meteorological Institute, Oslo.

Johnson, C., M. Inall, and S. Häkkinen (2013), Declining nutrient concentrations in the Northeast Atlantic as a result of a weakening subpolar gyre, *Deep Sea Res., Part I*, *82*, 95–107, doi:10.1016/j.dsr.2013.08.007.

Kanzow, T., et al. (2010), Seasonal variability of the Atlantic Meridional Overturning Circulation at 26.5°N, *J. Clim.*, *23*(21), 5678–5698, doi:10.1175/2010JCLI3389.1.

Karl, T. R., A. Arguez, B. Huang, J. H. Lawrimore, J. R. McMahon, M. J. Menne, T. C. Peterson, R. S. Vose, and H. Zhang (2015), Possible artifacts of data biases in the recent global surface warming hiatus, *Science*, *348*(6242), 1469–1472, doi:10.1126/science.aaa5632.

Katsman, C., and G. van Oldenborgh (2011), Tracing the upper ocean's "missing heat", *Geophys. Res. Lett.*, *38*, L14610, doi:10.1029/2011GL048417.

Kieke, D., and I. Yashayaev (2015), Studies of Labrador Sea water formation and variability in the subpolar North Atlantic in the light of international partnership and collaboration, *Prog. Oceanogr.*, *132*, 220–232, doi:10.1016/j.pocean.2014.12.010.

Kintisch, E. (2014), Into the maelstrom, *Science*, *344*(6181), 250–253, doi:10.1126/science.344.6181.250.

Kosaka, Y., and S. Xie (2013), Recent global-warming hiatus tied to equatorial pacific surface cooling, *Nature*, *501*(7467), 403–407, doi:10.1038/nature12534.

Larsen, K., H. Hátún, B. Hansen, and R. Kristiansen (2012), Atlantic water in the faroe area: Sources and variability, *ICES J. Mar. Sci.*, *69*, 802–808, doi:10.1093/icesjms/fss028.

Lee, S., W. Park, M. O. Baringer, A. L. Gordon, B. Huber, and Y. Liu (2015), Pacific origin of the abrupt increase in Indian Ocean heat content during the warming hiatus, *Nat. Geosci.*, *8*(6), 445–449, doi:10.1038/ngeo2438.

Levitus, S., J. Antonov, T. Boyer, R. Locarnini, H. García, and A. Mishonov (2009), Global ocean heat content 1955–2008 in light of recently revealed instrumentation problems, *Geophys. Res. Lett.*, *36*, L07608, doi:10.1029/2008GL037155.

Lozier, M. S., S. Leadbetter, R. G. Williams, V. Roussenov, M. S. C. Reed, and N. J. Moore (2008), The spatial pattern and mechanisms of heat-content change in the North Atlantic, *Science*, *319*, 800–803.

Mauritzen, C., A. Melsom, and R. Sutton (2012), Importance of density-compensated temperature change for deep North Atlantic Ocean heat uptake, *Nat. Geosci.*, *5*, 905–910, doi:10.1038/ngeo1639.

Meehl, G. A., J. M. Arblaster, J. T. Fasullo, A. Hu, and K. E. Trenberth (2011), Model-based evidence of deep-ocean heat uptake during surface-temperature hiatus periods, *Nat. Clim. Change*, *1*, 360–364, doi:10.1038/nclimate1229.

Meehl, G. A., A. Hu, J. Arblaster, J. Fasullo, and K. E. Trenberth (2013), Externally forced and internally generated decadal climate variability associated with the Interdecadal Pacific Oscillation, *J. Clim.*, *26*, 7298–7310, doi:10.1175/JCLI-D-12-00548.1.

Mercier, H., et al. (2013), Variability of the meridional overturning circulation at the Greenland-Portugal OVIDE section from 1993 to 2010, *Prog. Oceanogr.*, *132*, 250–261, doi:10.1016/j.pocean.2013.11.001.

Nieves, V., J. K. Willis, and W. C. Patzert (2015), Recent hiatus caused by decadal shift in Indo-Pacific heating, *Science*, *349*, 532–535, doi:10.1126/science.aaa4521.

Ollitrault, M., and J. Rannou (2013), ANDRO: An Argo-based deep displacement dataset, *J. Atmos. Oceanic Technol.*, *30*, 759–788.

Pingree, R. D. (1993), Flow of surface waters to the west of the British-Isles and in the Bay of Biscay, *Deep Sea Res., Part II*, *40*(1–2), 369–388.

Piron, A., V. Thierry, H. Mercier, and G. Caniaux (2015), Genesis and spatial extension of 1000m deep convection event in the Irminger Sea in 2011–2012 revealed by Argo floats. Geophysical Research Abstracts EGU2015-5991 presented at 2015 EGU General Assembly Vienna, Austria, 12–17 Apr.

Pollard, R. T., M. J. Griffiths, S. A. Cunningham, J. F. Read, F. F. Pérez, and A. F. Ríos (1996), Vivaldi 1991—A study of the formation, circulation and ventilation of eastern North Atlantic Central Water, *Prog. Oceanogr.*, *37*(2), 167–192.

Reid, J. L. (1994), On the total geostrophic circulation of the North Atlantic Ocean: Flow patterns, tracers, and transports, *Prog. Oceanogr.*, *33*, 1–92.

Roemmich, D., J. Church, J. Gilson, D. Monselesan, P. Sutton, and S. Wijffels (2015), Unabated planetary warming and its ocean structure since 2006, *Nat. Clim. Change*, *5*(3), 240–245, doi:10.1038/nclimate2513.

Sévellec, F., T. Huck, M. B. Jelloul, N. Grima, J. Vialard, and A. Weaver (2008), Optimal surface salinity perturbations of the meridional overturning and heat transport in a global ocean general circulation model, *J. Phys. Oceanogr.*, *38*(12), 2739–2754, doi:10.1175/2008JPO3875.1.

Shein, K. A. (2006), State of the climate in 2005, *Bull. Am. Meteorol. Soc.*, *87*, s1–s102, doi:10.1175/BAMS-87-6-shein.

Smeed, D. A., G. D. McCarthy, S. A. Cunningham, E. Frajka-Williams, D. Rayner, W. E. Johns, C. S. Meinen, M. O. Baringer, B. I. Moat, A. Duchez, and H. L. Bryden (2014), Observed decline of the Atlantic Meridional Overturning Circulation 2004–2012, *Ocean Sci.*, *10*(1), 29–38, doi:10.5194/os-10-29-2014.

Somavilla, R., C. González-Pola, C. Rodriguez, S. A. Josey, R. F. Sánchez, and A. Lavín (2009), Large changes in the hydrographic structure of the Bay of Biscay after the extreme mixing of winter 2005, *J. Geophys. Res.*, *114*, C01001, doi:10.1029/2008JC004974.

Somavilla, R., C. González-Pola, M. Ruiz Villarreal, and A. Lavín (2011), Mixed layer depth (MLD) variability in the southern Bay of Biscay. Deepening of winter MLDs concurrent to generalized upper water warming trends?, *Ocean Dyn.*, *61*(9), 1215–1235, doi:10.1007/s10236-011-0407-6.

Srokosz, M. A., and H. L. Bryden (2015), Observing the Atlantic Meridional Overturning Circulation yields a decade of inevitable surprises, *Science*, *348*(6241), 1255575, doi:10.1126/science.1255575.

Trenberth, K. E. (2015), Has there been a hiatus?, *Science*, *349*(6249), 691–692, doi:10.1126/science.aac9225.

Trenberth, K. E., and J. T. Fasullo (2010), Climate change: Tracking Earth's energy, *Science*, *328*(5976), 316–317, doi:10.1126/science.1187272.

Trenberth, K. E., J. T. Fasullo, G. Branstator, and A. S. Phillips (2014), Seasonal aspects of the recent pause in surface warming, *Nat. Clim. Change*, *4*, 911–916, doi:10.1038/nclimate2341.

Williams, R. G., V. Roussenov, D. Smith, and M. S. Lozier (2014), Decadal evolution of ocean thermal anomalies in the North Atlantic: The effect of ekman, overturning and horizontal transport, *J. Clim.*, *27*, 698–719, doi:10.1175/JCLI-D-12-00234.1.

Woollings, T. (2011), Atmospheric science: Ocean effects of blocking, *Science*, *334*(6056), 612–613, doi:10.1126/science.1214167.

Yashayaev, I., and J. W. Loder (2009), Enhanced production of Labrador Sea water in 2008, *Geophys. Res. Lett.*, *36*, L01606, doi:10.1029/2008GL036162.